Utilizing visible and near infrared spectroscopy based on multi-class support vector machines classification to characterize olive oil adulteration

Mahdi Ghasemi-Varnamkhasti[1*], Samaneh Amini-Pozveh[1], Seyed Ahmad Mireei[2], Puneet Mishra[3], Satyabrata Ghosh[4], Davoud Ghanbarian[1], Zahra Izadi[1]

(1. *Department of Mechanical Engineering of Biosystems, Shahrekord University, PO Box 115, Shahrekord 88186-34141, Iran*;
2. *Department of Biosystems Engineering, College of Agriculture, Isfahan University of Technology, Isfahan 84156-83111, Iran*;
3. *Department of Rural Engineering, Universidad Politecnica de Madrid (UPM), 28040, Madrid, Spain*;
4. *Department of Food Technology & Bio-Chemical Engineering, Jadavpur University, Kolkata-700032, India*)

Abstract: Rapid and non-destructive adulteration detection is of particular importance to oil industries. This paper presents an application of visible and near-infrared (VNIR) spectroscopy for detection of adulteration levels in olive oil. Sunflower oil was used as an adulterant to olive oil, and the adulteration samples with different levels ranging from 0% to 40% were prepared and used for the experiments. The spectra were first considered in the range of 500-900 nm and then smoothened and normalized to reduce the light scattering effects. Principal component analysis (PCA) was performed on the spectra to have a primary data visualization and feature extraction. The extracted PCA scores were used to calculate the Mahalanobis distances of the adulterated samples from the pure sample. Further, the PCA scores were fed to the multi-class support vector machine (SVM) model to perform classification on the basis of different adulteration levels. The results showed that the spectral normalization highlighted different regions over the spectrum affected due to the adulteration. The PCA score biplots showed differences in the samples based on the different amounts of the adulteration. Moreover, the Mahalanobis distance provided a quantitative measure of the differences between the adulterated oil and the pure oil samples. The SVM modelling further supported the classification of the different levels of the adulteration. Consequently, the VNIR spectroscopy in combination with the SVM could support the development of the classification protocols for detection of adulteration in olive oils.

Keywords: computer aided classification, spectroscopy, olive oil industry, Mahalanobis distance, support vector machine

Citation: Ghasemi-Varnamkhasti, M., S. Amini-Pozveh, S. A. Mireei, P. Mishra, S. Ghosh, D. Ghanbarian, and Z. Izadi, 2018. Utilizing visible and near infrared spectroscopy based on multi-class support vector machines classification to characterize olive oil adulteration. Agricultural Engineering International: CIGR Journal, 20(3): 206–214.

1 Introduction

Due to the increase in food fraud with adulteration methods and subsequently, the loss of large amounts of capital and consumer confidence, adulteration detection in foods through fast, accurate, and non-destructive techniques is significantly important (Manning and Soon, 2014). Vegetable oils are a group of foods which are not safe from adulteration (Jiménez-Carvelo et al., 2017). Among different vegetable oils, olive oil is involved in adulteration by cheaper and less nutritional value oils due to its importance in the diet and expense (Jabeur et al., 2016). Therefore, detection of adulteration in olive oil is one of the most important issues to determine its quality. Tests and procedures used for adulterations detection are usually destructive, time-consuming, and require a lot of expensive laboratory equipment (Santos et al., 2017).

One of the popular methods that can be employed as a non-destructive, rapid, and in an accurate way for

Received date: 2017-10-06 **Accepted date:** 2017-12-24

* **Corresponding author: Ghasemi-Varnamkhasti, G.,** Department of Mechanical Engineering of Biosystems, Shahrekord University, PO Box 115, Shahrekord 88186-34141, Iran. Tel/fax: +98-3832324428. Email: ghasemymahdi@gmail.com.

detection of adulteration is visible/near-infrared (VNIR) spectroscopy. The VNIR spectroscopy, as a cheap and fast method for determining the authenticity and adulteration detection, has shown promising results worldwide (Kamal and Karoui, 2015). Detection of food adulteration utilising VNIR has been reported previously in many cases. For instance, Alamprese et al. (2013) used ultraviolet (UV), Vis, near-infrared (NIR), and mid-infrared (MIR) for the detection of minced beef adulterated with turkey meat. In that study, 44 minced beef samples, 44 turkey meat samples, and 154 samples with the combination of both meat types were tested. Spectral data with different pre-processing methods were considered. The result of the data analysis in the visible range was relatively satisfactory even though the best result was obtained in NIR range. They concluded the fusion of the data in three ranges could result in the best classification accuracy (Alampress et al., 2013). Gayo et al. (2006) reported the use of VNIR technique for authenticity evaluation of crab meat. Partial least squares regression (PLSR) and principal component regression (PCR) were used as the chemometric approaches and both could detect the adulteration in crab meat with a similar performance. The standard error of prediction (SEP) obtained from PLS and PCR was 0.252 and 0.244, respectively. They suggested the VNIR technology could be successfully employed for authentic crab meat assessment (Gayo et al., 2006).

In the case of oil, even though there are some reports in the literature concerning NIR spectroscopy method for detecting adulteration (Gurdeniz and Ozen, 2009; Graham et al., 2012; Nunes, 2014; Wu et al., 2016), however, few studies have been reported yet on the use of VNIR combined with advanced chemometric strategy for evaluation of oil adulteration. One such study was performed by Downey et al. (2002) where VNIR spectroscopy was used to examine the adulteration of extra virgin olive oil (EVOO) with sunflower oil. In that study, 137 oil samples from eastern Mediterranean regions were considered. Soft independent modelling of class analogy (SIMCA) was used to classify the samples. Based on their results, the classification accuracy was 100% and 90% obtained from the first and second derivatives of spectra, respectively, in the wavelength range of 400-2498 nm (Downey et al., 2002).

Apart from oil adulteration detection using VNIR, some works concerning VNIR application to oil quality evaluation have been already reported (García Martín, 2015; Cayuela Sánchez et al., 2013; Giovenzana et al., 2015).

Advanced data analysis techniques have been developed so far as the substantial chemometric tools to analyse the multivariate data associated with the VNIR spectroscopy. Particularly for VNIR data, a useful chemometric strategy was reported by Wen et al. (2015) who investigated the presence of soybean and colza oils as adulterant materials in camellia oil samples. They employed competitive adaptive reweighted sampling (CARS) as variable selection method to extract the required information from the spectra. Furthermore, PLS was considered to establish the calibration models. In final, the performance of CARS was satisfactorily reported for the study aim (Wen et al., 2015). More recently, Xian et al. (2016) reported the chemometric methods including interval partial least squares (iPLS), synergy interval partial least squares (SiPLS), and backward interval partial least squares (BiPLS) to find the olive oil adulterated with deep frying oil using VNIR technique. The wavelength range was within 400-2500 nm. Based on the report, SiPLS and BiPLS showed the best results in adulteration detection (Xian et al., 2016).

According to the best our knowledge, no study has been reported yet on detecting the adulteration in olive oil using VNIR in the wavelength of 500-900 nm. The current study has been fulfilled this aim by employing an advanced chemometric strategy to extract the most appropriate information from the obtained spectra. The methodology first performed the spectral pre-processing to enhance the information present in the data. Later, principal component analysis (PCA) was used to explore the data and extract the features based on the variance explained by the data. Further, to quantify the differences in the adulterated oil and the pure one, the PCA scores were used to calculate the Mahalanobis distances. To perform classification, the PCA scores were used for multi-class support vector machines (SVMs). The results showed that VNIR in combination with SVM could be

used to develop the classification protocols for olive oils adulteration.

2 Materials and methods

2.1 Sample preparation

A total of six bottles of virgin olive oil, which all were prepared from Tarom, a northern region in Iran, were considered. Oil extraction had already been performed in Roodbar, a northern region in Iran. From each bottle, nine samples were taken for conducting the experiments. Adulteration levels were considered as zero, 5%, 10%, 20%, 30%, and 40% by using sunflower oil. Since the purpose of adulteration is being economic in order to reducing the costs, the original sunflower oil was not used and the adulteration was applied by a type of sunflower oil on the market. At each level of adulteration, considering six bottles of oil and nine replicates for each bottle, 54 spectrum data were obtained. During the test, oils were kept at a constant temperature room and were then prepared in the volume of 10 mL of tubes for sampling.

2.2 NIR measurement

In the present research, a spectrometer (model: Compact, LASERTACK Co., Canada) was used to collect the spectra of the oil samples in transmission mode of measurement. The spectrometer could acquire the spectra of the samples within 200-1100 nm with the wavelength and board resolutions of 1 nm and 16 bit, respectively. A precise grating has been used in the spectrometer to isolate the wavelengths onto the detector. The detector of the spectrometer was a CCD array (model: TOSHIBA TCD 1305 AP) with a number of pixel of 3648. Using a cuvette holder accessory, the spectrometer could ideally acquire the absorption spectra of the liquid samples such as oils. The cuvette holder had been equipped with a 10 W tungsten/halogen lamp which could produce a consistent illumination for the samples using a 15 V power supply. The light passed the path of 12 mm after entering the cuvette through the optical port and then, entered into the spectrometer via SMA 905 standard port. Before acquiring the sample spectra, reference and dark measurements were conducted for calculating the relative spectra. Then, without changing the position of the cuvette, 5 mL of the sample was poured into the cuvette and the raw, absorption, and transmission spectra were recorded for each sample. The scan number and the integration time of the spectrometer were set as x and y, respectively. After collecting each sample spectrum, the cuvette was washed and well cleaned and the entire process was repeated from the beginning of the next sample.

2.3 Chemometric strategy

2.3.1 Spectral pre-processing

The data acquired with spectroscopy techniques usually contains non-chemical biases such as changing the detector sensitivity, scattering effects, and interferences from external light sources. Therefore, data pre-processing in spectroscopy is an important step, before performing any advanced chemometric data analysis.

Due to the low detector sensitivity in the extreme region of spectral bands, the wavelength range was reduced from 200-1000 nm to 500-900 nm. Further, to reduce the noises at the local level over the spectrum, smoothening with the help of Savitzky-Golay (SAVGOL) algorithm was performed. The SAVGOL smoothening was performed with the help of a 15-point window and the second order polynomial. Furthermore, to reduce any baseline shift and variations due to global signal intensity, the standard normal variates (SNV) were calculated for each spectrum. All the further data analysis was performed by using the pre-processed spectra.

2.3.2 PCA

PCA is the most popular data visualisation and feature extraction technique commonly used in spectroscopy domain (Wold et al., 1987). The major aim of the PCA is to identify the major independent sources of variation in the data which can support an enhanced visualisation of the data. Typically, in the case of spectroscopy data, the major sources are the wavelength regions of the spectrum which are causing variation in the data. Implementation of PCA involves performing orthogonal transformation of the correlated wavelengths to linearly uncorrelated variables defined as the principal components (PCs). Retaining the maximum amount of the variability in the data is the major aim of this data transformation. Further, the order of the PCs extracted from the data defines the amount of variability explained in the data i.e., the first PC represent the maximum amount of variability, the

second PC explains the most of the left variability (orthogonal of the first two PCs) and so on. The PCA decomposition model for spectra set matrix $X(n \times p)$ can be understood as Equation (1):

$$X = TW^T \quad (1)$$

where, T is the score in lower explained by the number of principal components specified and W is a $p \times p$ matrix whose columns are the eigenvectors of X^TX.

The number of extracted PCs defines the new orthonormal basis set for the data and later that can be used to perform the data visualisation. To have an interpretation of data in two or three-dimensional plots, the respective PCs can be selected and defined as the new orthonormal basis set for the data to perform the transformation. The transformation of data based on PCs can be performed as follow (Equation (2)):

$$\hat{X} = XW \quad (2)$$

where, $\hat{X}$ is the score in lower explained by the number of principal components specified, $X(n \times p)$ is the mean centred original data matrix, and W is a $p \times p$ matrix whose columns are the eigenvectors of X^TX.

2.3.3 Mahalanobis distance

Mahalanobis distance is the high dimension Euclidean distance (Mahalanobis, 1936). The only difference is the covariance matrix used in the case of Mahalanobis which is usually unity in the case of Euclidean distance. Typically, it is a multi-dimensional generalisation for measuring the number of standard deviation that away from some distribution. The calculation of Mahalanobis distances can be understood as Equation (3):

$$D = \sqrt{(x-m)^T S^{-1}(x-m)} \quad (3)$$

where, D is the Mahalanobis distance; m is the mean spectral profile of the pure oil samples, and S is the covariance matrix for the pure oil spectra.

2.3.4 Multi-class support vector machine

Adulteration detecting problems usually involve assigning a particular label to the oil samples such as adulterated or not adulterated, which can typically be understood as a binary class assignment. Further, when there are different levels of adulteration in the sample, the case extends from binary class to multi-class. SVM are powerful supervised non-probabilistic learning data modelling techniques popular for performing both binary and multi-class classification tasks (Cortes and Vapnik, 1995). The SVM utilises the hyper-planes to define decision boundaries between classes for performing the classification. Further, to deal with the non-linear complex nature of the data, SVM utilises kernel functions to map the data to a higher-dimension, where it can be linearly separated with the help of hyper-planes. The choice of the hyper-planes is made in such a way that they allow the largest margin for separation of the classes. The SVM algorithms are usually developed to perform a binary classification, however, SVM can be used for multi-class classification problems by utilising several independent binary classifiers. This can be performed by combining it with ensemble methods such as error correcting output codes (ECOC). The ECOC deals with the multi-class classification problem by converting it into several independent binary classification problems (Übeyli, 2007).

In the present work, two different classification experiments were performed. One was a multi-class classification for identifying different levels of adulteration in the olive oils ranging from 0%-40% and leading to a five-class classification problem. The second classification experiment was performed for classifying two different range of adulteration 0%-10% and 20%-40%, leading to a two-class binary classification problem. For both cases, the SVM modelling utilises the Matlab's Statistics and Machine Learning Toolbox (R2016b). For the multi-class modelling a cubic SVM was used and for the binary problem a linear SVM was used. The ECOC-SVM uses a one-versus-one coding design, in which for each binary learner, one class was assigned a positive value and the other was assigned a negative value. The coding design utilises all combinations of class pairs assignment. To map the data to the higher dimension, a Radial Basis Function (RBF) kernel was used. RBF kernel has the benefit of non-linearly mapping the sample to the higher dimensional space for dealing with a non-linear relationship between observations and classes. The cross-validation of the model was performed by 10-fold cross-validation method. In this method, the calibration data is divided into 10 equal parts. For making the model, 9 out of 10 parts were used to cross-validate, the 10^{th} part

was used to test. This was repeated for 10 times and the average prediction accuracy was recorded. The trained classifier characteristics were then presented with the cross-validation accuracy, receiver operator characteristics (ROC) curves, and confusion matrix.

3 Results and discussion

3.1 Spectral profiles

Figure 1 presents the mean spectral profile of the six different olive oils used in the experiment. Further, Figure 1(a) explains the mean raw absorbance profile and Figure 1(b) presents the mean spectrum profile after the pre-processing with SAVGOL and SNV methods. It can be seen clearly in Figure 1(a) that before the pre-processing, the oil spectra are differing in their global intensities and thus, the comparison is a difficult task. However, after the pre-processing, the spectra become much more similar and the difference due to global intensities is now eliminated. The correction is possible with the help of SNV transformation which reduced the spectra to a zero mean and unit standard deviation. Over the spectrum at various waveband regions, different peaks could be identified in the wavebands of 540-550 nm, 550-570 nm, 600-630 nm, and 650-689 nm. Different peaks correspond to different biochemical components presented in the olive oils. In the previous works, different peaks in the similar regions had been identified due to the fluorescence molecules presented in the oils. The major fluorescent molecules exhibited characteristic signatures at different wavelengths such as chlorophylls and pheophytins (600-750 nm), compounds derived from vitamin E (~525 nm), and primary and secondary oxidation products (485-540 nm) (Kyriakidis and Skarkalis, 2000).

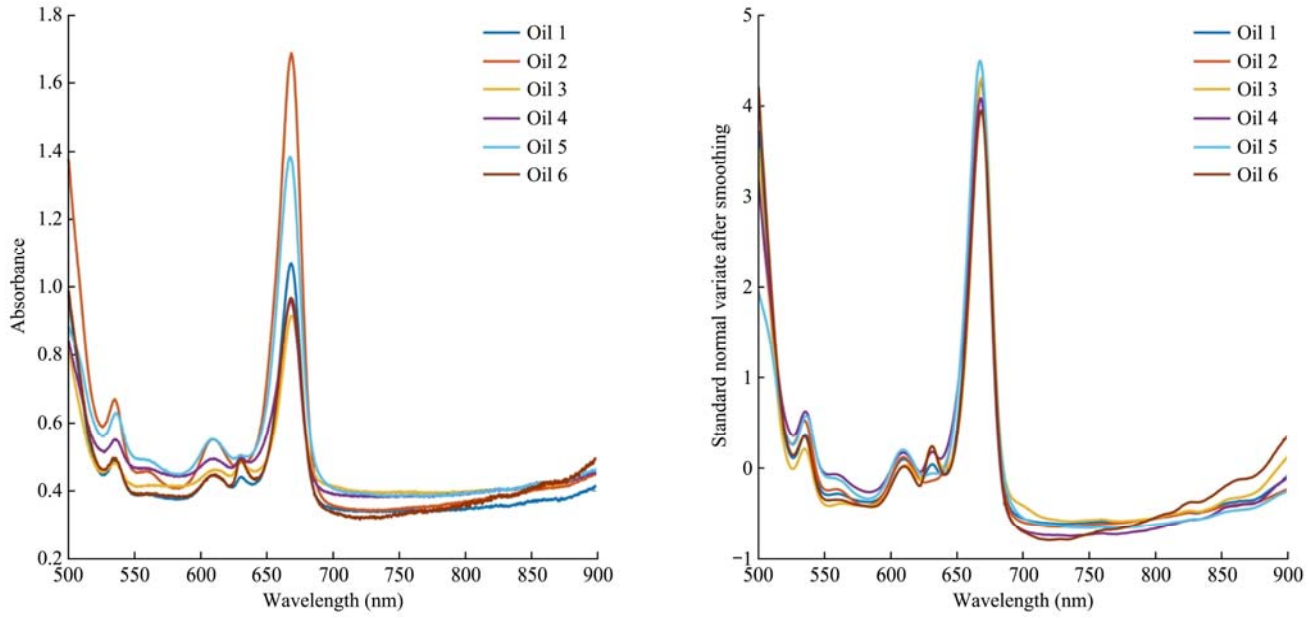

(a) Mean raw absorbance profiles (b) Mean Spectral profiles after preprocessing with SNV and SAVGOL smoothing

Figure 1 Mean spectral profiles of six olive oil samples

Figure 2 presents the spectra of an olive oil adulterated at different levels of adulteration, ranging from 0%-40%. The presented spectra were smoothened and normalised. Over the spectrum, it could be clearly seen that different regions over the spectrum exhibited difference in signal intensities. This differences in intensities could be understood as resulting from the differences in the levels of adulteration, as the differences due to global intensities were reduced with the help of pre-processing. The major differences could be identified in the regions from 520-640 nm, 700-900 nm, and the peak at 670 nm. The difference could have raised due to the differences in the chemical composition of the sunflower oil. Increasing amount of adulteration affected the spectral profile of olive oils and more characteristics dominated by sunflower when the amount of adulteration was increasing. It could also be seen that in the region of 800-900 nm, the adulteration from 0%-10% and 20%-40% identified as two separate cases.

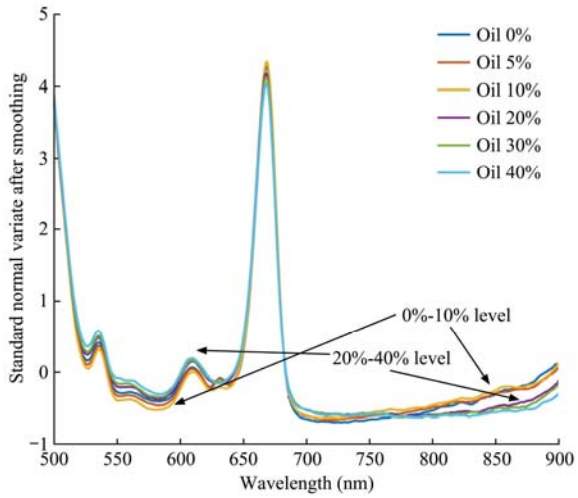

Figure 2 Preprocessed spectral profiles of olive oil for different levels of adulteration 0% (dark blue), 5% (red), 10% (Yellow), 20% (Purple), 30% (Green) and 40% (Sky blue)

3.2 PCA

A total of 8 PCs were selected from the data based on the 98.63% of explained variance. Figure 3 further depicts the criteria (cumulative variance explained) and evolution of the variance as the PCs were extracted. Figure 4, further presents the loading and the scores resulting from the first 3 PCs explaining a total of 89.66% of the data variance. The Figure 4 (a, b, c) presents the loading and the Figure 4 (d, e, f) presents the scores corresponding to the loadings. The loading of the first PC had two different major peaks at 620 nm and 670 nm, which could be understood as the result of the pheophytins and chlorophyll presented in the oils. The second and the third PCs had the peaks at various different locations but independent to each other. For the second PC, a high-intensity broad peak could be seen in the region of 700-800 nm, whereas, for the PC3, various different peaks could be identified. In the score plots, it could be seen clearly that the major differences identified

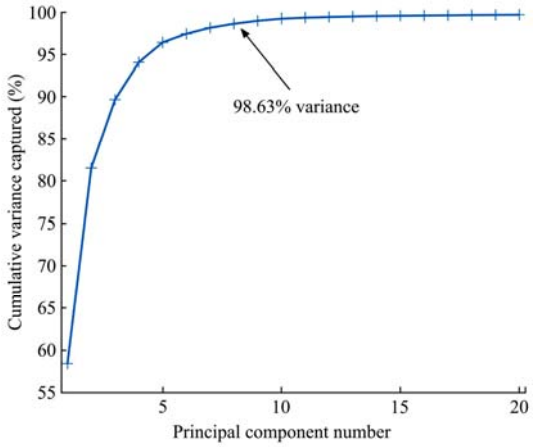

Figure 3 Criterion for selecting the number of principal components, cumulative variance captured versus the number of principal components extracted

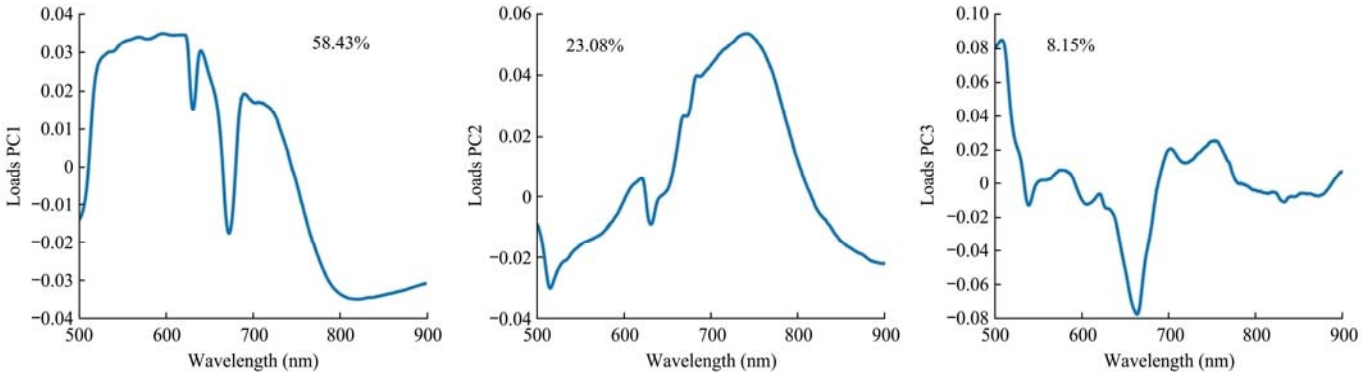

(a) First loading

(b) Second loading

(c) Third loading

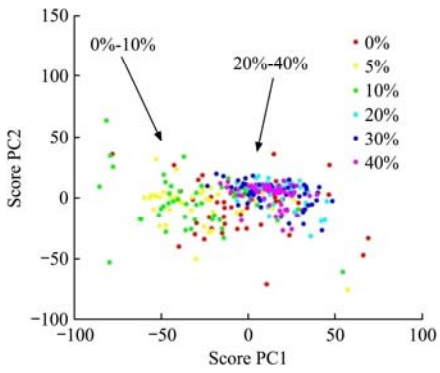

(d) First vs second PC scores

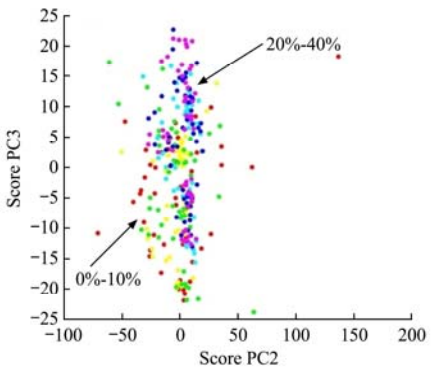

(e) Second vs third PC scores

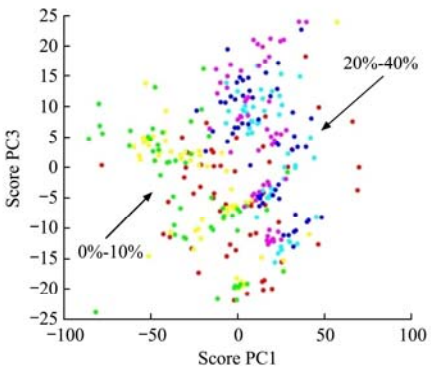

(f) First vs third PC scores

Figure 4 The loading and scores of first three principal components capturing 89.66% of total variance in the data

in the score were obtained from the different amount of adulteration ranges. Two major clusters could be identified, one belonging to the adulteration level from 0%-10%, and the other for the adulteration level of 20%-40%. However, it was difficult to identify visually and comment on any particular oil, because the experiment was performed with repetition and consisting of a large number of oil samples.

3.3 Mahalanobis distances

Figure 5 presents the Mahalanobis distance plot for the adulterated oil samples. The x- and y axes explain the sample and Mahalanobis distance from the pure oil, respectively. A zero distance indicated the pure olive oil sample. The different levels of adulteration could be identified with different markers. It could be seen in Figure 5 that globally for all the oil samples, the Mahalanobis distance was greater than zero, and no sample was identified as the pure olive oil sample, which was in accordance, since all the samples presented were adulterated oil samples. Further, it could be seen that as the amount of adulteration was increasing, the Mahanalobis distance was also increasing, highlighting the dissimilarity in the adulterated oil and pure oil samples. However, this increase was not the same for all the olive oils. In some oils (Oil samples of 1, 3, 4, and 6), the distance increased rapidly, whereas in the case of other oil samples (Oil samples of 2 and 5), the distance was evolving slowly.

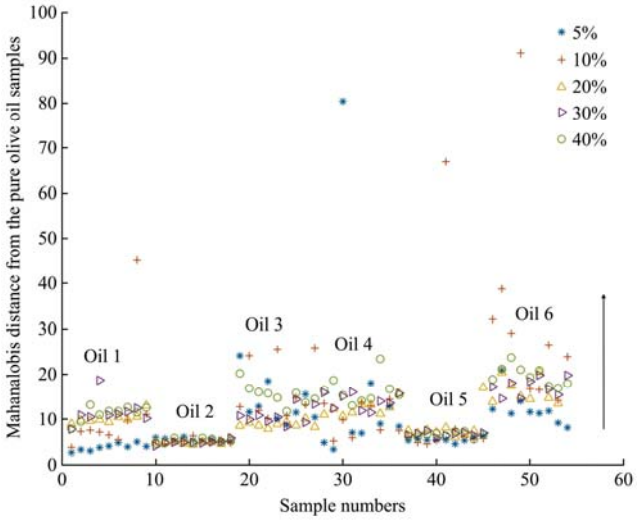

Figure 5 Mahanalobis distance of adulterated oil samples (5%-40%) from the pure oil samples based on the first 8 PC scores

3.4 Classification results

Figure 6 and 7 present the results of two different SVM classification models developed for classifying different levels of adulteration range from 0%-40% and also, for classifying the two different levels range of adulteration 0%-10% and 20%-40%. For both cases, the performance of the models was presented with the help of ROC curves and the confusion matrices. It could be seen clearly in Figure 6 that it was difficult for the model to classify accurately the different levels of adulteration in

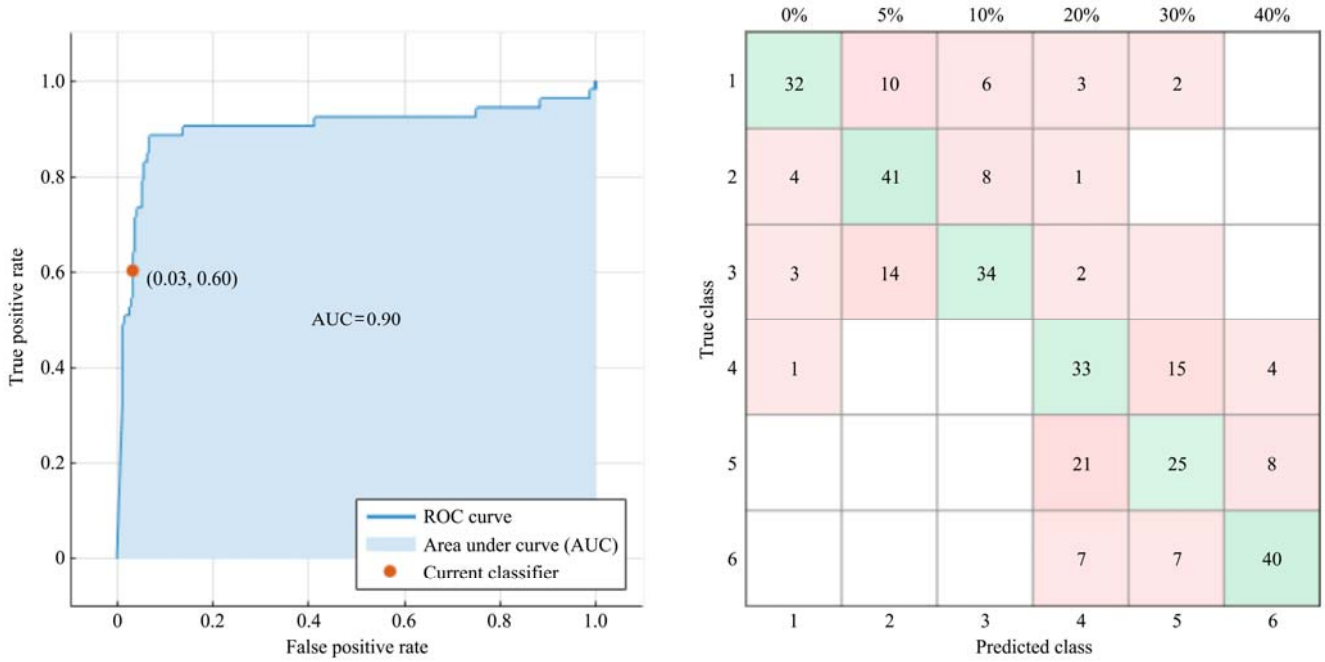

Figure 6 ROC characteristic and the confusion matrix for the SVM model developed for the classification of different levels of adulteration in olive oil samples (0%-40%)

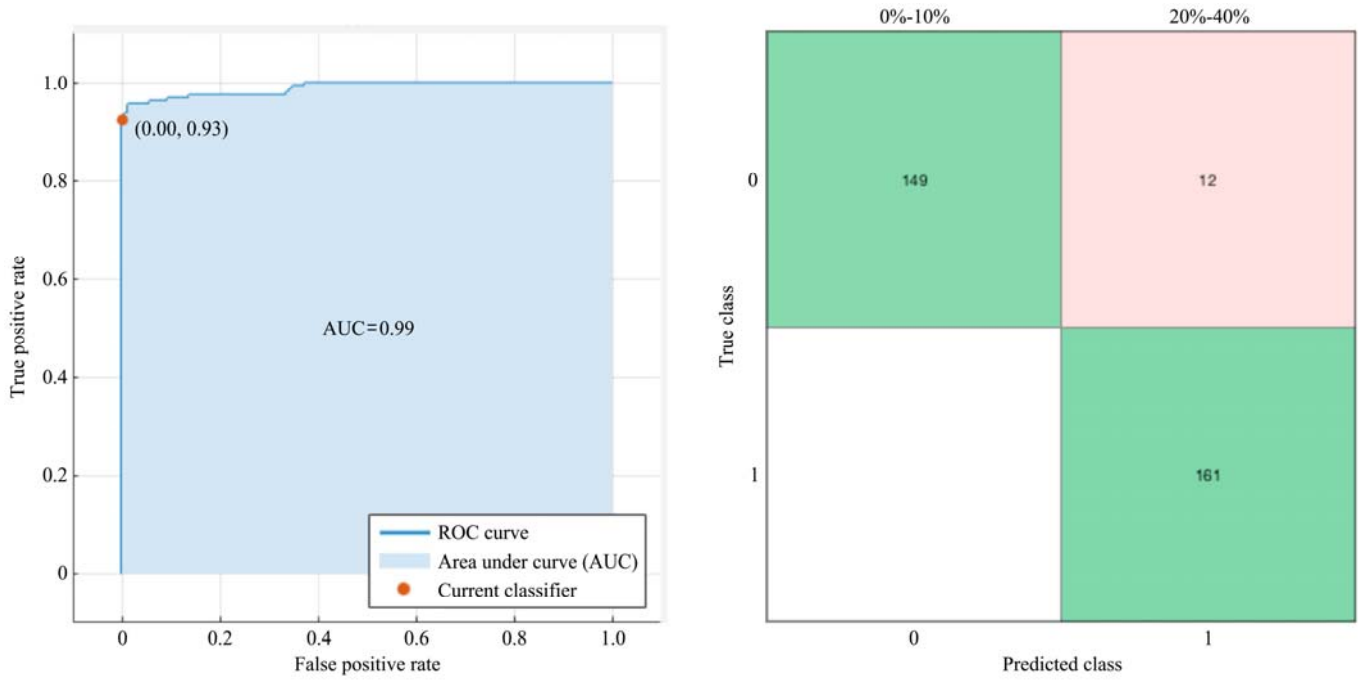

Figure 7 ROC characteristic and the confusion matrix for the SVM model developed for the classification of olive oil samples adulterated with 0%-10% from 20%-40% adulterated samples

oil samples. As a result of which, a high misclassification for different classes was obtained. However, the overall validation accuracy of the model for a 10-fold cross validated calibration model was 62.1%. For the binary classification case, the performance of the SVM was very high as compared to the multi-class classification of adulteration levels of the olive oils. It could also be seen in Figure 7, that only 12 samples were misclassified. The overall accuracy of the model was 96.3%. A reason or the poor performance of the multi-class model could be understood as very similar spectral profiles of the samples for the low level of adulteration, especially for <10%. Furthermore, the variability of different olive oils used altogether for modelling complicated the model and led to a misclassification case.

4 Conclusion

Non-destructive and rapid detection of adulteration in olive oils is a major concern for the industry as well as for consumers. The present study was implemented to investigate the potential of VNIR spectroscopy and SVM classification for detecting different levels of adulteration of sunflower oil in olive oil. The effect of adulteration was identified at different locations over the VNIR spectrum. Further, the PCA and Mahalanobis distance supported the visualisation of multivariate data generated by the VNIR. The accuracy of SVM model was 62.1% for classifying the different levels of adulteration in oils and 96.3% for detecting the adulteration in the range of 0%-10% and 20%-40%. VNIR spectroscopy could support the detection of sunflower oil adulteration in olive oil, however, study showed that detecting lower levels (<10%) of adulteration was a challenging task for VNIR spectroscopy.

References

Alamprese, C., M. Casale, N. Sinelli, S. Lanteri, and E. Casiraghi. 2013. Detection of minced beef adulteration with turkey meat by UV–vis, NIR and MIR spectroscopy. *LWT-Food Science and Technology*, 53(1): 225–232.

Cayuela Sánchez, J. A., W. Moreda, and J. M. García. 2013. Rapid determination of olive oil oxidative stability and its major quality parameters using Vis/NIR transmittance spectroscopy. *Journal of Agricultural and Food Chemistry*, 61(34): 8056–8062.

Cortes, C., and V. Vapnik. 1995. Support vector machine. *Machine Learning*, 20(3): 273–297.

Downey, G., P. McIntyre, and A. N. Davies. 2002. Detecting and quantifying sunflower oil adulteration in extra virgin olive oils from the Eastern Mediterranean by visible and near-infrared spectroscopy. *Journal of Agriculture and Food Chemistry*, 50(20): 5520–5525.

García Martín, J. F. 2015. Optical path length and wavelength selection using Vis/NIR spectroscopy for olive oil's free

acidity determination. *International Journal of Food Science and Technology*, 50(6): 1461–1467.

Gayo, J., S. A. Hale, and S. M. Blanchard. 2006. Quantitative analysis and detection of adulteration in crab meat using visible and near-infrared spectroscopy. *Journal of Agriculture and Food Chemistry*, 54(4): 1130–1136.

Giovenzana, V., R. Beghi, R. Civelli, S. Marai, and R. Guidetti. 2015. Postharvest characterization of olive oil fruits texture by NIR and vis/NIR spectroscopy. *Chemical Engineering Transactions*, 44: 61–66.

Graham, S. F., S. A. Haughey, R. M. Ervin, E. Cancouët, S. Bell, and C. T. Elliott. 2012. The application of near-infrared (NIR) and Raman spectroscopy to detect adulteration of oil used in animal feed production. *Food Chemistry*, 132(3): 1614–1619.

Gurdeniz, G., and B. Ozen. 2009. Detection of adulteration of extra-virgin olive oil by chemometric analysis of mid-infrared spectral data. *Food chemistry*, 116(2): 519–525.

Jabeur, H., A. Zribi, and M. Bouaziz. 2016. Extra-virgin olive oil and cheap vegetable oils: distinction and detection of adulteration as determined by GC and chemometrics. *Food Analytical Methods*, 9(3): 712–723.

Jiménez-Carvelo, A. M., M. T. Osorio, A. Koidis, A. González-Casado, and L. Cuadros-Rodríguez. 2017. Chemometric classification and quantification of olive oil in blends with any edible vegetable oils using FTIR-ATR and Raman spectroscopy. *LWT-Food Science and Technology*, 86: 174–184.

Kamal, M., and R. Karoui. 2015. Analytical methods coupled with chemometric tools for determining the authenticity and detecting the adulteration of dairy products: A review. *Trends in Food Science and Technology*, 46(1): 27–48.

Kyriakidis, N. B., and P. Skarkalis. 2000. Fluorescence spectra measurement of olive oil and other vegetable oils. *Journal of AOAC International*, 83(6): 1435–1439.

Mahalanobis, P. C. 1936. On the generalised distance in statistics. Proceedings of the National Institute of Sciences of India. 1936, 49–55.

Manning, L., and J. M. Soon. 2014. Developing systems to control food adulteration. *Food Policy*, 49: 23–32.

Nunes, C. A. 2014. Vibrational spectroscopy and chemometrics to assess authenticity, adulteration and intrinsic quality parameters of edible oils and fats. *Food Research International*, 60: 255–261.

Santos, P. M., F. V. C. Kock, M. S. Santos, C. M. S. Lobo, A. S. Carvalho, and L. A. Colnago. 2017. Non-invasive detection of adulterated olive oil in full bottles using time-domain NMR relaxometry. *Journal of the Brazilian Chemical Society*, 28(2): 385–390.

Übeyli, E. D. 2007. ECG beats classification using multiclass support vector machines with error correcting output codes. *Digital Signal Processing*, 17(3): 675–684.

Wen, Z., T. Sun, P. Xu, and M. Liu. 2015. Adulteration detection of camellia oils by Vis/NIR spectroscopy and variable selection method. *Journal of Jiangsu University (Natural Science Edition)*, 36(6): 673–678.

Wold, S., K. Esbensen, and P. Geladi. 1987. Principal component analysis. *Chemometrics and Intelligent Laboratory Systems*, 2(1-3): 37–52.

Xian, R., F. Huang, Y. Li, S. Pan, Z. Chen, Z. Chen, and Y. Wang. 2016. Quantitative analysis of deep-frying oil adulterated virgin olive oil using Vis-NIR spectroscopy with iPLS, *Spectroscopy and Spectral Analysis*, 36(8): 2462–2467.